SLOPE STABILITY ANALYSIS USING FINITE ELEMENT METHOD ON TEPUS-JERUKWUDEL ROAD

Dian Rusmanawati[1]*, I Gede Budi Indrawan[2], Hendy Setiawan[3]

[1]Department of Geological Engineering, Universitas Gadjah Mada, Yogyakarta, 55284, Indonesia

e-mail:dianrusma@mail.ugm.ac.id[1]

ABSTRACT
Tepus-Jerukwudel Road construction is one of the South Coast Java Road sections located in Gunungkidul Regency, Special Region of Yogyakarta. One of the hills with the deepest excavation depth is at STA 14+350. The research location includes the Punung Formation which is dominated by reef limestones. The existing rock lithology is floatstone. The depth of the road excavation is more than 20 meters. The slope design is 3V:1H. This research aimed to analyze the slope stability of the Tepus-Jerukwudel Road and assess the safety factor of the slope design. We used the finite element method (FEM) in the Rocscience Phase2 v8.0 software by applying the Generalized Hoek-Brown method for the rock failure criteria. The loads considered in the slope stability analysis were live loads, dead loads, surcharge loads, and seismic loads. The results of the slope analysis without seismic loads resulted in the safety factor values for the left and right slopes of 4,49 and 3,32, respectively. For seismic loads conditions, the safety factor values for the left and right slopes are 3,74 and 2,66. The results indicated that slope design of the road is in a stable condition in accordance with the estimated static and seismic loads.

Keywords: Finite element method; Safety factor; Slope stability.

INTRODUCTION
The Tepus-Jerukwudel Road is one of the South Coast Java Road sections. South Coast Java Road is expected to be a transportation solution from the congested North Coast Java Road to switch to the southern route. The Tepus-Jerukwudel road is located in the Pegunungan Seribu area, Gunungkidul Regency, at coordinates 110º38'57.6" east longitude 8º07'51.9" south latitude. The research location includes the Punung Formation, which is dominated by limestone reefs. One of the difficulties in constructing this road segment is rock excavation work with a depth of more than 20 meters. This high rock excavation will likely cause landslides during construction and post-construction. One of the hills with the deepest excavation is at STA 14+350. The depth on the left side is 20,299 meters and on the right side is 37,000 meters. The slope design by Special Region of Yogyakarta National Road Planning and Supervising Working Unit (2020) is 3V:1H. Slope stability analysis is used to determine the safety factor of slope design. It is based on the results of geological investigations, such as investigations of morphology, lithology, rocks, groundwater, seismicity, and classification of rock mass strength. Slope stability analysis using the finite element method with Rocscience Phase2 v8.0 software.

This research aimed to analyze the slope stability of the Tepus-Jerukwudel Road and assess the safety factor of the slope design using finite element method. The research results are expected to provide input to stakeholders regarding slope stability and road construction so that road construction can be carried out more efficiently and precisely.

The lithology at research area rocks is limestone. The Dunham Classification is the most widely used scheme for the description of limestone in the field. The primary criterion used in this

Accepted: 30 July 2022

classification scheme is the texture, which is described in terms of the proportion of carbonate mud present and the framework. Figure 1 shows The Dunham classification of carbonate sedimentary rocks with modifications.

Slope stability is assessed by comparing shear strength (cohesion and friction angle), defined as the ratio of resisting forces (working load) to driving forces (collapse load) (Komadja et al., 2020). The slope is considered stable if the resisting force is greater than the driving force. The ratio of resisting forces to driving forces is known as the safety factor which characterises the stability of the slope (Bishop, 1955; Bushira et al., 2018; Pradhan et al., 2014; Raghuvanshi, 2019; Renani & Martin, 2020). The slope stability analysis was conducted using the Finite Element Method (FEM). Fundamental to the assessment of slope stability by finite element methods (FEM) is the strength reduction finite element method (Dyson & Tolooiyan, 2018; Sun et al., 2016). The shear strength reduction approach includes the search for a stress/strength reduction factor (SRF) value that brings the slope to fail (You et al., 2018). The safety factor is equal to the strength reduction factor when a collapse occurs. The slope stability was analyzed using the Rocscience Phase2 v8.0 software for conditions with and without seismic loads. The critical value of SRF/safety factor, maximum shear strain, and total displacement was obtained using the Rocscience Phase2 v8.0 software. The safety factor is shown by the critical value of the SRF, the slip surface by the maximum shear strain value, and the total displacement value by the most considerable slope displacement value. The recommended safety factor value refers to SNI 8460:2017, where the slope condition is said to be stable if it has a safety factor value of more than 1.10 for states with seismic loads and more than 1.50 for states without seismic loads.

The slope stability analysis parameters for the Generalized Hoek-Brown failure criteria consist of four parameters (Rocscience, 2007) as follows:

1. Unconfined compressive strength of intact rock (σ_{ci}), which is obtained from the results of the compressive strength test of rock. The compressive strength of intact rock is the most significant parameter used for the characterization of intact rock (Teymen & Mengüç, 2020).
2. Intact rock parameter (m_i), represents the rock masses with different degree of hardness. It is obtained from the table presented by Hoek (2007) in (Zuo & Shen, 2020) as in Table 1.
3. Geological Strength Index (GSI), is used to determine rock mass characterization based on field observations including geological data on rock mass. The Geological Strength Index (GSI) used for this study is classified by Marinos (2010).
4. Disturbance factor, is a factor depending on the degree of influence to which the rock mass has been subjected to the blast damage and stress relaxation due to excavation. The disturbance factor value refers to Hoek & Brown (2019).

According to Belghali & Saada (2018), the loads imposed on the slopes are self weight, surcharge, and seismic forces. In road construction, traffic loads need to be imposed, so that the loads considered in the slope stability analysis are as follows:

1. The live loads calculated for the analysis are the traffic loads. The traffic loads are added to the entire width of the road surface, which is determined based on the road class as presented in Table 2.

Accepted: 30 July 2022

2. The dead loads calculated in the slope stability analysis are the self-weight of this slope.
3. The surcharge load applied on the top surface of the slope is 10 kN/m2 as shown in Table 2.
4. Seismic loads have a significant impact and can be the primary cause of slope collapse in seismically active locations (Xu & Yang, 2018). According to SNI 8460:2017, the seismic design for the excavated slope has a 2% chance of exceeding its magnitude over a 50-year design life, which corresponds to a 500-year return time. The peak acceleration on the ground surface (A_s) is the earthquake parameter used in the design analysis. The horizontal seismic coefficient (kh) was determined to be 0.5 of the horizontal peak acceleration by determining the site class and amplification factor.

   The A_s value is obtained by multiplying the PGA (peak ground acceleration) value by the amplification factor according to the type of soil at the research site (can be seen in Table 3 and Table 4) according to the following equation:

   $A_s = F_{pga} \times PGA$

   where A_s is the seismic design peak acceleration coefficient, F_{pga} is the site coefficient for bedrock peak acceleration, and PGA is peak ground acceleration.

METHODS

The research method was carried out by determining the research location, identifying problems, literature review, collecting primary data, secondary data, and slope stability analysis. Primary data collection is done by direct observation on rock slopes. Laboratory tests were performed on rock samples, including the rock physical properties test and the Uniaxial Compressive Strength (UCS) test. Secondary data are core drill results, seismic data, and slope geometry design. Slope stability analysis using finite element method in the Rocscience Phase2 v8.0 software. The rock mass is assumed to be homogeneous and isotropic, so the strength of the rock mass is modelled using the Generalized Hoek-Brown failure criteria. The weathering rate and the rock mass quality are considered to be continuous horizontally into the slope. Parameters for slope stability analysis using Rocscience Phase2 v8.0 software are rock specific gravity, elastic properties and rock mass strength. Parameters of elastic properties include Poisson's ratio and Young's Modulus. The rock strength parameters for the Generalized Hoek-Brown criteria include the value of Uniaxial Compressive Strength (UCS), GSI value, Intact Rock Constant mi, and disturbance factor (D) which can then be calculated for parameter values of mb, s, and a. The value of the specific gravity of the rock is obtained from the mechanical properties test of the rock. The value of UCS, Poisson's ratio, and Young's Modulus were obtained from the compressive strength test of rocks. Figure 2 shows the research method.

RESULTS AND DISCUSSION

Based on the Geological Map of the Bantul-Wonosari Region by Surono (2009), the research location is in the Punung Formation. According to Husein & Srijono (2007) in Choanji (2017), the research location is part of a limestone hill with steep slopes. According to the observations of geological surface conditions and examination of the rock descriptions results, it is known that the rock types are limestone floatstone Nichols (2009). Floatstone is white, with occasional marine fossils larger than 2 mm visible in some locations, and matrix-supported.

Accepted: 30 July 2022

The GSI classified by Marinos (2010) is used for the classification of surface rock masses. Surface GSI values range from 45 to 65 (type A, fair weathering). Figure 3 shows three sets of discontinuities with good interlocking conditions, rough rock surface conditions, and moderate weathering in floatstone limestone. Figure 4 illustrates an analysis of rock mass quality using the GSI method at STA 14+350.

The slope design is designed by Special Region of Yogyakarta National Road Planning and Supervising Working Unit (2020) with a ratio 3V:1H or 71.56º. Slopes are made by making benches at every five meters height. The bench is made with a width of 1.5 meters with a bench slope ratio of 10V:1H or 5.71º. The left slope height is 20.299 meters with three benches and the right slope height is 37.000 meters with seven benches. Based on the core data, at depths up to 35 meters, the groundwater level has not been found so the groundwater level is not calculated in this analysis. Because the disturbances caused by rock slope excavation at the location are relatively minor, the disturbance factor value for rock slope excavation is zero. Figure 5 illustrates the slope design. Table 5 shows the parameters required for FEM slope stability analysis using Rocscience Phase2 v8.0 software.

The loading data included in the software are as follows:

1. The live loads are the traffic loads according to Table 2, for road class I, the traffic loads are 15 kPa.
2. The dead loads are self weight, for the floatstone has a specific gravity of 2,19 gr/cm^3.
3. The surcharge loads on the slope surface are 10 kPa.
4. Seismic loads are calculated according to the research location. Based on the bedrock peak acceleration map (SB) for probabilistic exceeding 10% within 50 years (National Earthquake Study Center, 2017), it shows that the research location is 0.25-0.3g. The peak acceleration value used was 0.3g. Site classification was determined based on the NSPT value of the rock. Based on the results of the NSPT test on the core drill, the NSPT value is more than 60. Based on Table 4 the amplification factor for PGA and a period of 0.2 seconds (AASHTO, 2012), the site classification belongs to the SC site class (hard soil, very dense, and soft rock). The amplification factor for the PGA value of 0.3g SC site class was 1.1. Thus, the value of the seismic peak acceleration coefficient is:
   $$A_s = F_{pga} \times PGA$$
   $$= 1.1 \times 0.3 = 0.33$$
   The horizontal seismic coefficient (kh) was determined to be 0.5 of the horizontal peak acceleration by determining the site class and amplification factor. It means that the seismic loads value for slope stability analysis is 0.33 × 0.5 = 0.165.

Based on the slope stability analysis results with FEM on the Tepus-Jerukwudel STA 14+350 road in Figure 6 and 8, the safety factor with seismic loads on the left slope is 3.74, and the right slope is 2.66. This value has above the 1.10 safety factor requirement. The safety factor without seismic loads on the left slope is 4.49 and on the right slope is 3.32. This value has above the 1.50 safety factor requirement. It means that the slope conditions are stable. Table 6 shows a recapitulation of the safety factor.

Table 6 shows that the safety factor is lower in states with seismic loads than without seismic loads. Slope stability analysis result using FEM without

Accepted: 30 July 2022

seismic loads have a higher safety factor than with seismic loads. It means that the seismic loads causes a decrease in the value of the safety factor (Karrech et al., 2022; Zaei & Rao, 2017). The highest shear strain value can be used to determine the mechanism of slope failure and the position of the slip surface. The slip surface is located at the bottom of the excavation boundary or bottom of the bench.

As shown in Table 7, Figure 7, and Figure 9, the total displacement value for condition without seismic loads on the left slope is 0.52 mm and the right slope is 1.40 mm, while the total displacement value for condition with seismic loads on the left slope is 0.69 mm and the right slope is 1.80 mm. The total displacement value meets the criteria of one meter maximum displacements on rock slopes under seismic load condition (Hyness-Griffin et al., 1984 in Duncan dkk., 2014). The total displacement value with seismic loads is higher than without seismic loads. It shows that the seismic loads affects the slope stability.

CONCLUSIONS

The slope stability analysis results using FEM show that the slope design is in a stable condition, both in states without seismic loads and with seismic loads. The total displacement value meets the maximum displacement requirements on the rock slopes. The safety factor value from the analysis using FEM shows a value that is much greater than the permit threshold. Further research is needed to determine the optimization by increasing the slope angle so that construction work is more efficient in terms of cost, time, and energy.

ACKNOWLEDGEMENT

The authors would like to acknowledge the Center for Implementation of National Roads for Central Java and Special Region of Yogyakarta for providing secondary data and granting permission to collecting the primary data.

REFERENCES

AASHTO. (2012). *LRFD Seismic Bridge Design Published by the American Association of State Highway and Transportation Officials*.

Belghali, M., & Saada, Z. (2018). Seismic Stability Analysis of Rock Slopes by Yield Design Theory Using The Generalized Hoek-Brown Criterion. *MATEC Web of Conferences*, *149*, 1–5. https://doi.org/10.1051/matecconf/201714902026

Bishop, A. W. (1955). The Use of The Slip Circle in The Stability Analysis of Slopes. *Geotechnique 5*, *5*(1), 7–17.

Bushira, K. M., Gebregiorgis, Y. B., Verma, R. K., & Sheng, Z. (2018). Cut Soil Slope Stability Analysis Along National Highway at Wozeka–Gidole Road, Ethiopia. *Modeling Earth Systems and Environment*, *4*(2), 591–600. https://doi.org/10.1007/s40808-018-0465-6

Choanji, T. (2017). Slope Analysis Based On SRTM Digital Elevation Model Data: Study Case On Rokan IV Koto Area And Surrounding. *Journal of Dynamics*, *1*.

Duncan, J. M., Wright, S. G., & Brandon, T. L. (2014). *Soil Strength and Slope Stability, Second Edition*. John Wiley & Sons.

Dyson, A. P., & Tolooiyan, A. (2018). Optimisation of Strength Reduction Finite Element Method Codes for Slope Stability Analysis. *Innovative Infrastructure Solutions*, *3*(1), 38.

Accepted: 30 July 2022

https://doi.org/10.1007/s41062-018-0148-1

Hoek, E., & Brown, E. T. (2019). The Hoek–Brown Failure Criterion and GSI – 2018 Edition. *Journal of Rock Mechanics and Geotechnical Engineering*, *11*(3), 445–463. https://doi.org/10.1016/j.jrmge.2018.08.001

Husein, S., & Srijono. (2007). Tinjauan Geomorfologi Pegunungan Selatan DIY/Jawa Tengah : Telaah Peran Faktor Endogenik dan Eksogenik dalam Proses Pembentukan Pegunungan. *Https://Www.Researchgate.Net/Publication/282946295*. https://doi.org/10.13140/RG.2.1.2784.0727

Karrech, A., Dong, X., Elchalakani, M., Basarir, H., Shahin, M. A., & Regenauer-Lieb, K. (2022). Limit analysis for the seismic stability of three-dimensional rock slopes using the generalized Hoek-Brown criterion. *International Journal of Mining Science and Technology*, *32*(2), 237–245. https://doi.org/https://doi.org/10.1016/j.ijmst.2021.10.005

Komadja, G. C., Pradhan, S. P., Roul, A. R., Adebayo, B., Habinshuti, J. B., Glodji, L. A., & Onwualu, A. P. (2020). Assessment of stability of a Himalayan road cut slope with varying degrees of weathering: A finite-element-model-based approach. *Heliyon*, *6*(11). https://doi.org/10.1016/j.heliyon.2020.e05297

Marinos, V. (2010). New Proposed GSI Classification Charts for Weak or Complex Rock Masses. *Bulletin of the Geological Society of Greece*, *43*. https://doi.org/10.12681/bgsg.11301

National Earthquake Study Center. (2017). *Peta Sumber dan Bahaya Gempa Indonesia Tahun 2017*. Ministry of Public Works and Housing.

Nichols, G. (2009). *Sedimentologi and Stratigraphy Second Edition*. Willey-Blackwell.

Pradhan, S. P., Vishal, V., Singh, T. N., & Singh, V. K. (2014). Optimisation of Dump Slope Geometry Vis-à-vis Flyash Utilisation Using Numerical Simulation. *American Journal of Mining and Metallurgy*, *2*(1), 1–7. https://doi.org/10.12691/ajmm-2-1-1

Raghuvanshi, T. K. (2019). Plane Failure in Rock Slopes – A Review on Stability Analysis Techniques. *Journal of King Saud University - Science*, *31*(1), 101–109. https://doi.org/10.1016/j.jksus.2017.06.004

Renani, H. R., & Martin, C. D. (2020). Factor of Safety of Strain-Softening Slopes. *Journal of Rock Mechanics and Geotechnical Engineering*, *12*(3), 473–483. https://doi.org/10.1016/j.jrmge.2019.11.004

Rocscience. (2007). *User's Guide: RocLab Rock Mass Strength Analysis Using The Hoek-Brown Failure Criterion*. Rocscience Inc.

Sun, C., Chai, J., Xu, Z., Qin, Y., & Chen, X. (2016). Stability Charts for Rock Mass Slopes Based on The Hoek-Brown Strength Reduction Technique. *Engineering Geology*, *214*, 94–106. https://doi.org/10.1016/j.enggeo.2016.09.017

Surono. (2009). Litostratigrafi Pegunungan Selatan Bagian Timur Daerah Istimewa Yogyakarta dan

Accepted: 30 July 2022

Jawa Tengah. *Jurnal Geologi Dan Sumberdaya Mineral*, *19*(3), 209–221.

Teymen, A., & Mengüç, E. C. (2020). Comparative Evaluation of Different Statistical Tools for The Prediction of Uniaxial Compressive Strength of Rocks. *International Journal of Mining Science and Technology*, *30*(6), 785–797. https://doi.org/https://doi.org/10.1016/j.ijmst.2020.06.008

Xu, J., & Yang, X. (2018). Seismic Stability Analysis and Charts of a 3D Rock Slope in Hoek–Brown Media. *International Journal of Rock Mechanics and Mining Sciences*, *112*, 64–76. https://doi.org/https://doi.org/10.1016/j.ijrmms.2018.10.005

You, G., Mandalawi, M. Al, Soliman, A., Dowling, K., & Dahlhaus, P. (2018). Finite Element Analysis of Rock Slope Stability Using Shear Strength Reduction Method. *Sustainable Civil Infrastructures*, *1*, 227–235. https://doi.org/10.1007/978-3-319-61902-6_18

Zaei, M. E., & Rao, K. S. (2017). Evaluating the Effect of Strong Earthquake on Slope Instability. *Procedia Engineering*, *173*, 1771–1778. https://doi.org/https://doi.org/10.1016/j.proeng.2016.12.217

Zuo, J., & Shen, J. (2020). *The Hoek-Brown Constant mi*. https://doi.org/10.1007/978-981-15-1769-3_5

Accepted: 30 July 2022

Appendix

Table 1. Estimated m_i values for sedimentary rocks (Zuo & Shen, 2020)

Class	Group	Texture			
		Coarse	**Medium**	**Fine**	**Very Fine**
Clastic		Conglomerates (21±3) Breccias (19±5)	Sandstones (17±4)	Siltstones (7±2) Greywackes (18±3)	Claystones (4±2) Shales (6±2) Marls (7±2)
Non-clastic	Carbonates	Crystaline Limestone (12±3)	Sparitic Limestone (10±2)	Micritic Limestone (9±2)	Dolomites (9±3)
	Evaporites		Gypsum (8±2)	Anhydrite (12±2)	
	Organic				Chalk (7±2)

Table 2. Traffic loads for stability analysis and off-road loads by DPU (2001) in SNI 8460:2017

Road Class	Traffic Load (kPa)	Off Road Load (kPa)
I	15	10
II	15	10
III	12	10

Table 3. Site classification (AASHTO, 2012)

Site class	$\bar{v}_s$ (m/detik)	$\bar{N}_{SPT}$ or	$\bar{S}_u$ (kPa)
SA (hard rock)	> 1500	N/A	N/A
SB (rock)	750 to1.500	N/A	N/A
SC (hard soil, very dense and soft rock)	350 to 750	> 50	≥ 100
SD (medium soil)	175 to 350	15 to 50	50 to 100
SE (soft soil)	< 175	< 15	< 50
	Or any soil profile containing more than 3 m of soil with the following characteristics: 1. Plasticity index, PI >20, 2. Moisture content, $w \geq 40\%$, 3. Shear strength $\bar{S}_u$< 25 kPa		
SF (special soils, which require specific geotechnical investigations and site-specific response analysis)	Any subsoil profile that has one or more of the following characteristics: - Vulnerable and potentially fail or collapse due to earthquake loads such as easy liquefaction, very sensitive clay, weak cemented soil - Highly organic clay and/or peat (H > 3 m thick) - Very high plasticity clay (H thickness > 7.5 m with PI plasticity index > 75) - Soft/semi-firm clay layer with thickness H > 35 m with $\bar{S}_u$> 50 kPa		

Table 4. Amplification factors for PGA and 0.2 second period (F_{pga} and F_a) (AASHTO, 2012)

Site class	PGA ≤ 0,1	PGA = 0,2	PGA = 0,3	PGA = 0,4	PGA ≥ 0,5
Hard Rock (SA)	0,8	0,8	0,8	0,8	0,8
Rock (SB)	1,0	1,0	1,0	1,0	1,0

Accepted: 30 July 2022

Hard Soil (SC)	1,2	1,2	1,1	1,1	1,1
Medium Soil (SD)	1,6	1,4	1,2	1,1	1,0
Soft Soil (SE)	2,5	1,7	1,2	0,9	0,9
Special Soil (SF)	SS	SS	SS	SS	SS

Note: For intermediate values, linear interpolation can be performed

Table 5. Parameters of FEM slope stability analysis at STA 14+350

No	**Description**	**Unit**	**Lithology**
			Floatstone
1	Specific Gravity	gr/cm^3	2.19
		MN/m^3	0.02148
2	*Poisson's Ratio*		0.23
3	*Young's Modulus*	MPa	8,052.06
4	*UCS*	MPa	18.43
5	*GSI*		55
6	*Intact Rock Constant (mi)*		10
7	*Disturbance factor (D)*		0

Table 6. The results of slope stability analysis (safety factor) using FEM at STA 14+350

No	**Location**	**Condition**	**Safety Factor**	**Safety Factor Requirements**
1	Left slope	without seismic loads	4.49	1.50
		with seismic loads	3.74	1.10
2	Right slope	without seismic loads	3.32	1.50
		with seismic loads	2.66	1.10

Table 7. Total displacement with FEM at STA 14+350

No	**Location**	**Condition**	**Total Displacement**	
			(m)	**(mm)**
1	Left slope	without seismic loads	0.00052	0.52
		with seismic loads	0.00069	0.69
2	Right slope	without seismic loads	0.0014	1.40
		with seismic loads	0.0018	1.80

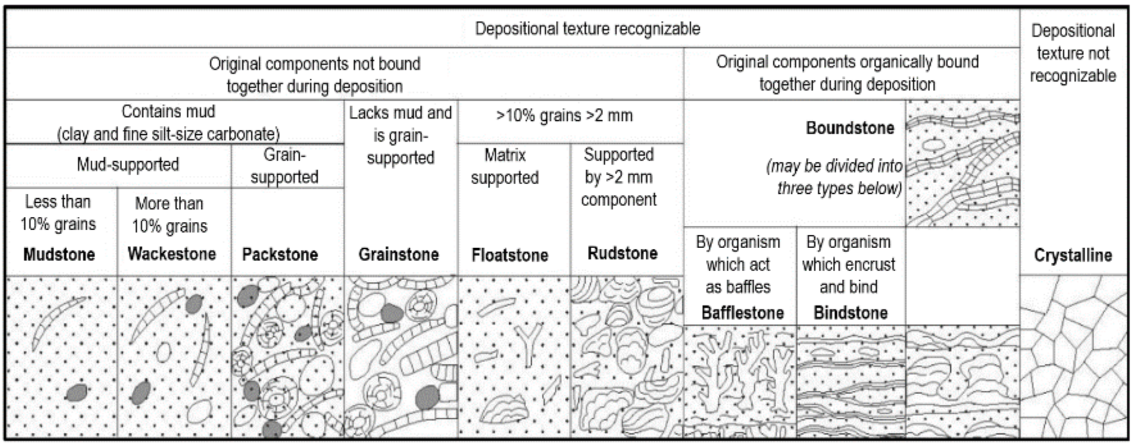

Figure 1. Dunham (1962) limestone classification was modified by Embry & Klovan (1971) and James & Bourque (1992) in Nichols (2009)

Accepted: 30 July 2022

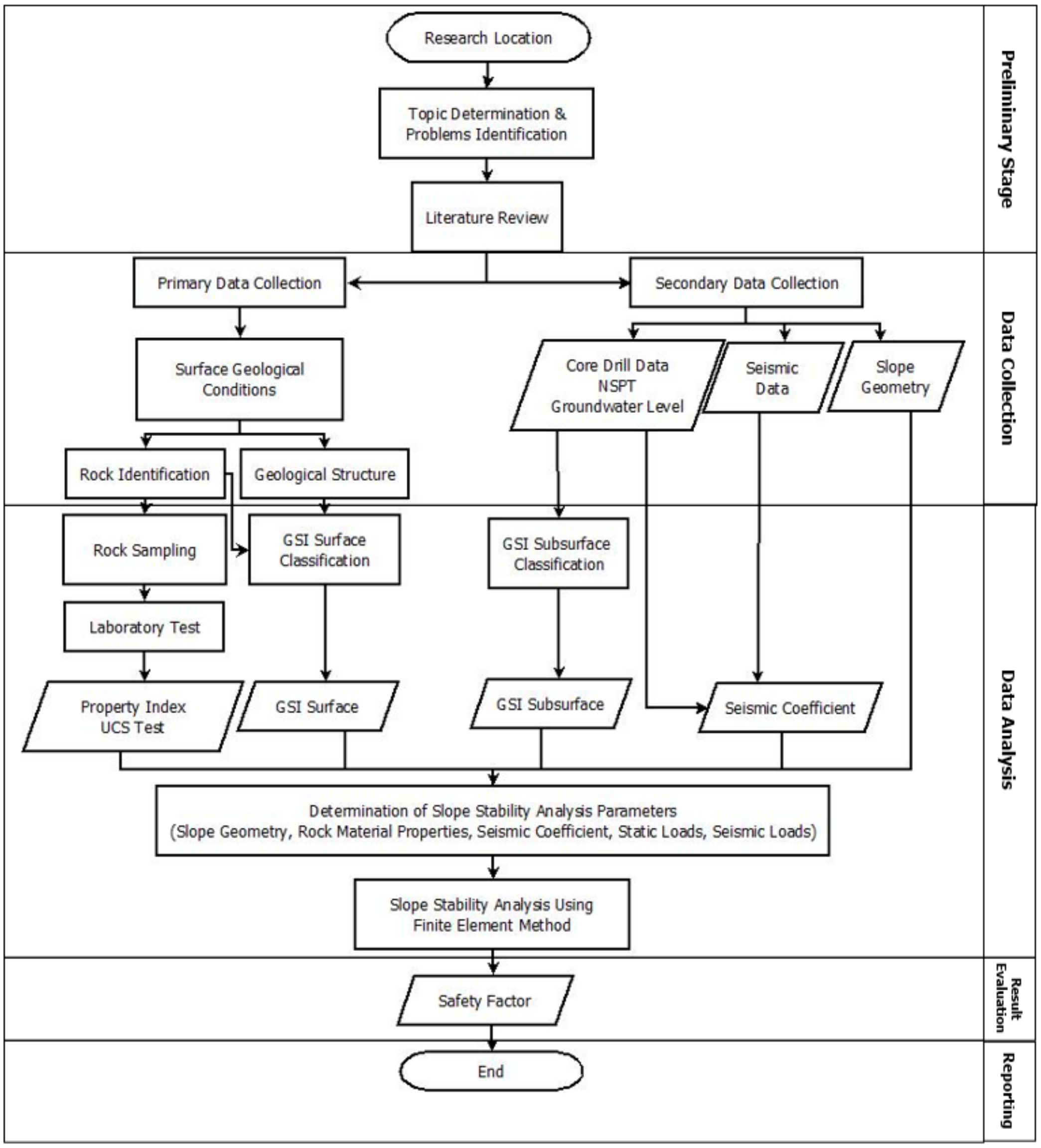

Figure 2. Flowchart of research

Accepted: 30 July 2022

Figure 3. Condition of floatstone rock mass structure (slope facing north): moderate weathering level, type A rock mass structure and composition, good rock mass condition, GSI value 45-65

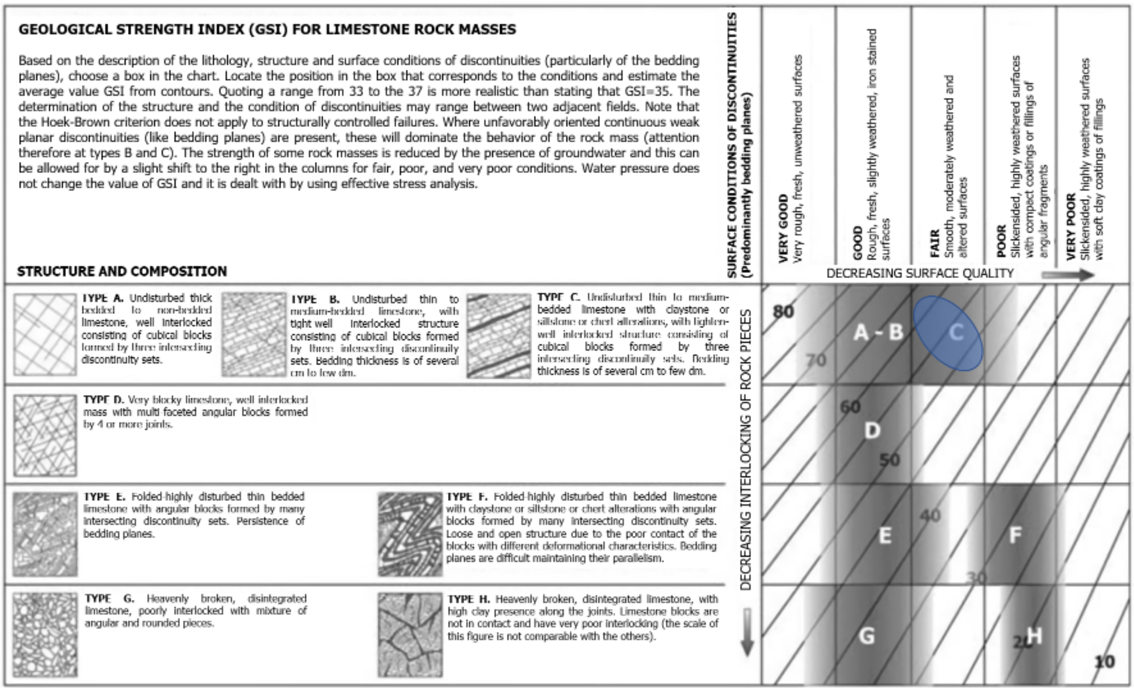

Figure 4. GSI surface analysis at STA 14+350

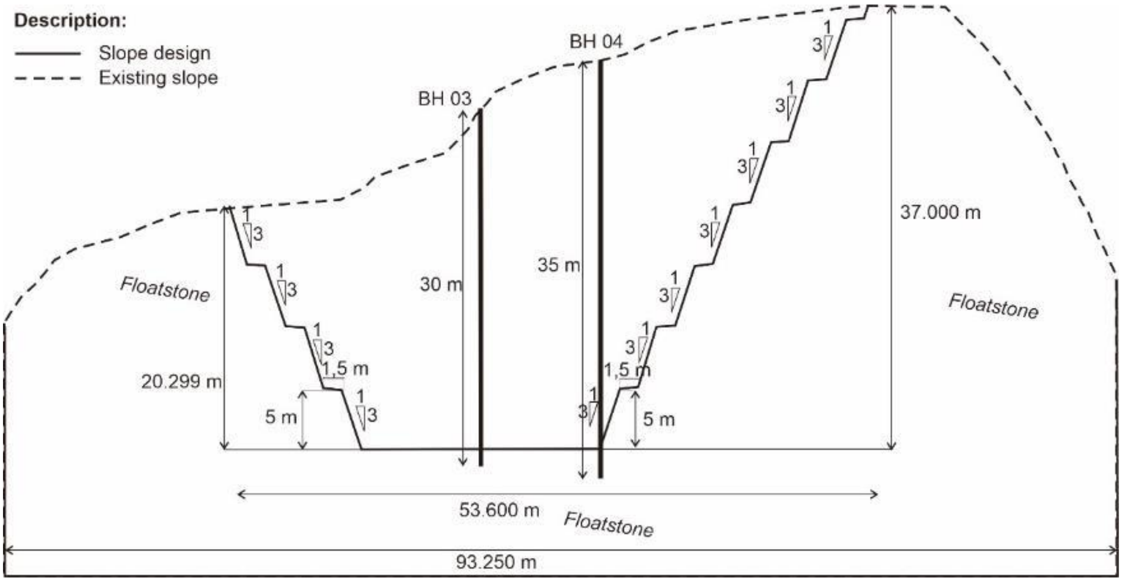

Figure 5. Slope modeling at STA 14+350

Accepted: 30 July 2022

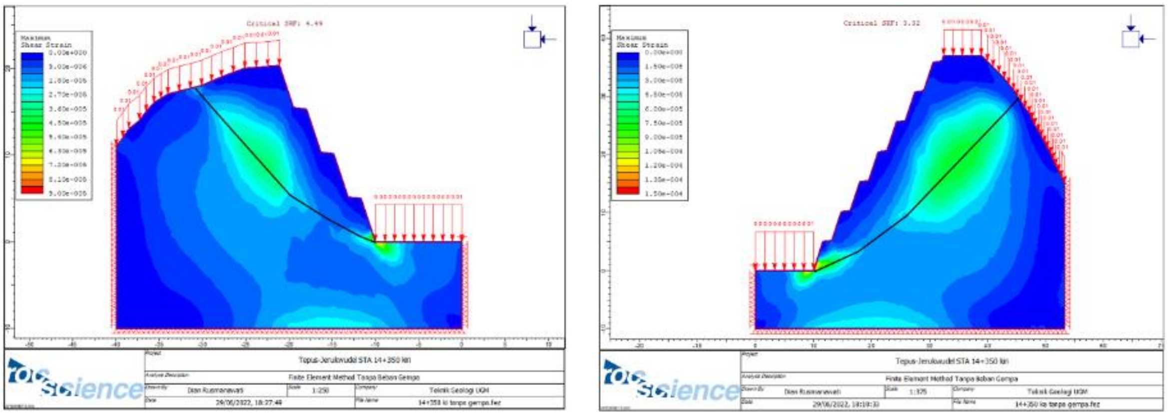

(a) (b)

Figure 6. The slope stability analysis results without seismic loads

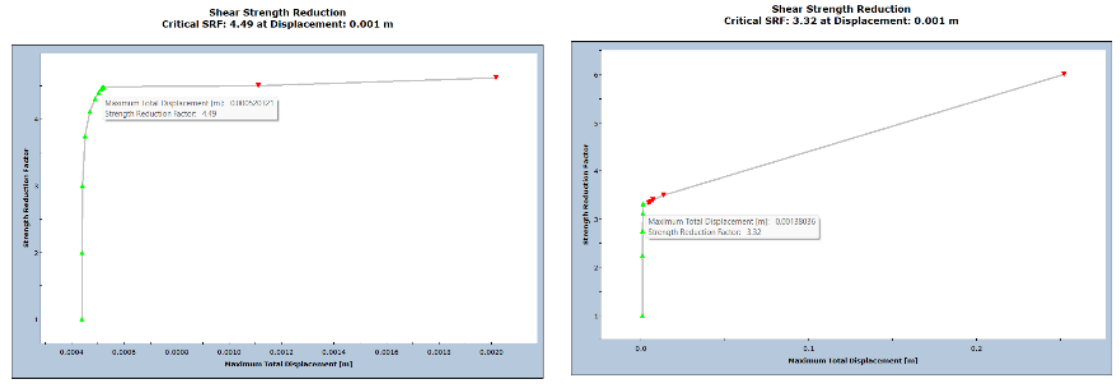

(a) (b)

Figure 7. Displacement graph without seismic loads

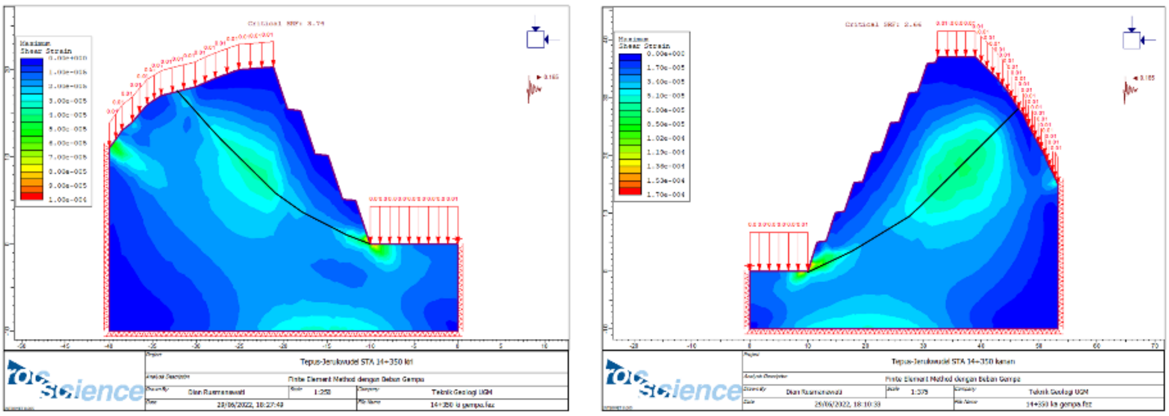

(a) (b)

Figure 8. The slope stability analysis results with seismic loads

Accepted: 30 July 2022

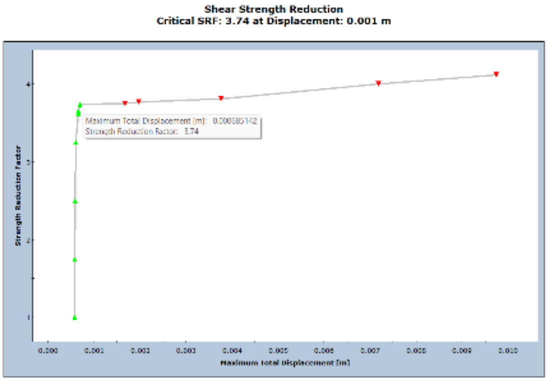

(a)

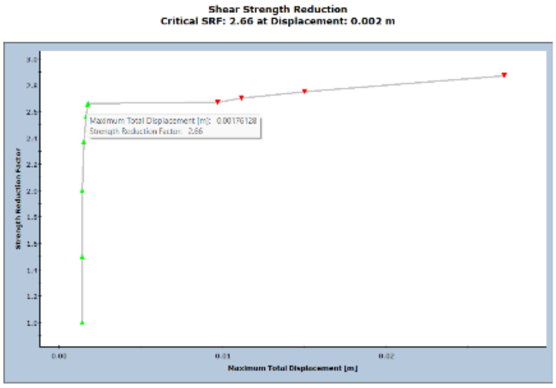

(b)

Figure 9. Displacement graph with seismic loads

Accepted: 30 July 2022